Title

Accelerated epigenetic aging in adolescents from low-income households is associated with altered development of brain structures

Journal

Metabolic Brain Disease, 35(8)

ISSN

0885-7490

Authors

Hoare, Jacqueline
Stein, Dan J
Heany, Sarah J
et al.

Publication Date

2020-12-01

DOI

10.1007/s11011-020-00589-0

Peer reviewed

HHS Public Access

Author manuscript

Metab Brain Dis. Author manuscript; available in PMC 2021 December 01.

Published in final edited form as:

Metab Brain Dis. 2020 December ; 35(8): 1287–1298. doi:10.1007/s11011-020-00589-0.

Accelerated epigenetic aging in adolescents from low-income households is associated with altered development of brain structures

Jacqueline Hoare, MD, PhD[1], **Dan J. Stein, MD, PhD**[2,3], **Sarah J. Heany, PhD**[2], **Jean-Paul Fouche, PhD**[2], **Nicole Phillips, MSocSci**[2], **Sebnem Er, PhD**[4], **Landon Myer, MD, PhD**[5,6], **Heather J. Zar, MD PhD**[7,8], **Steve Horvath, PhD**[9,10], **Andrew J. Levine, PhD**[3,11]

[1]Department of Psychiatry and Mental Health, University of Cape Town, Groote Schuur Hospital, Observatory, Cape Town, 7925, South Africa

[2]Department of Psychiatry and Mental Health, University of Cape Town, Groote Schuur Hospital, Observatory, Cape Town, 7925, South Africa

[3]SA MRC Unit on Risk & Resilience in Mental Disorders, Cape Town, South Africa

[4]Department of Statistics, University of Cape Town, Rondebosch, Cape Town, South Africa

[5]Centre for Infectious Disease Epidemiology and Research, School of Public Health & Family Medicine, University of Cape Town, Cape Town, South Africa

[6]Division of Epidemiology and Biostatistics, School of Public Health & Family Medicine, University of Cape Town, Cape Town, South Africa

[7]Department of Paediatrics and Child Health, Red Cross War Memorial Children's Hospital, Cape Town, South Africa

[8]SA Medical Research Council Unit on Child and Adolescent Health, Cape Town, South Africa

[9]Human Genetics, David Geffen School of Medicine, University of California Los Angeles, Los Angeles, CA, 90095, USA

[10]Biostatistics, School of Public Health, University of California Los Angeles, Los Angeles, CA, 90095, USA

Corresponding author and address for reprints: Prof Jacqueline Hoare, hoare.jax@gmail.com, Tel: 0027 21 4042134, Fax: 0027 214488158, Division of Liaison Psychiatry, Department of Psychiatry and Mental Health, University of Cape Town, Anzio Road Observatory, 7925, Cape Town, South Africa.

Author contributions

AJL, JH, DJS, and SH conceived of the study. AJL and JH are the PI's of the R21 which primarily funded this study. HZ is PI of the CTAAC study, from which most of the data were derived. SJH and SE carried out the statistical analysis. JF extracted the brain imaging data. JH wrote the first draft of the article. The remaining authors conceived of and aided with the CTAAC study, including collection of the DNA samples and phenotypic data. All authors helped in the interpretation of the findings and the write up of the article.

Potential conflicts of interest

All authors: No reported conflicts.

[11]Department of Neurology, David Geffen School of Medicine at the University of California, Los Angeles, CA, USA

Abstract

The relationship between cognitive performance, macro and microstructural brain anatomy and accelerated aging as measured by a highly accurate epigenetic biomarker of aging known as the epigenetic clock in healthy adolescents has not been studied. Healthy adolescents enrolled in the Cape Town Adolescent Antiretroviral Cohort Study were studied cross sectionally. The Illumina Infinium Methylation EPIC array was used to generate DNA methylation data from the blood samples of 44 adolescents aged 9 to 12 years old. The epigenetic clock software and method was used to estimate two measures, epigenetic age acceleration residual (AAR) and extrinsic epigenetic age acceleration (EEAA). Each participant underwent neurocognitive testing, T1 structural magnetic resonance imaging (MRI), and diffusion tensor imaging (DTI). Correlation tests were run between the two epigenetic aging measures and 10 cognitive functioning domains, to assess for differences in cognitive performance as epigenetic aging increases. In order to investigate the associations of epigenetic age acceleration on brain structure, we developed stepwise multiple regression models in R (version 3.4.3, 2017) including grey and white matter volumes, cortical thickness, and cortical surface area, as well as DTI measures of white matter microstructural integrity. In addition to negatively affecting two cognitive domains, visual memory (p=.026) and visual spatial acuity (p=.02), epigenetic age acceleration was associated with alterations of brain volumes, cortical thickness, cortical surface areas and abnormalities in neuronal microstructure in a range of regions. Stress was a significant predictor (p=.029) of AAR. Understanding the drivers of epigenetic age acceleration in adolescents could lead to valuable insights into the development of neurocognitive impairment in adolescents.

Keywords

DNA methylation; epigenetic clock; MRI; DTI; adolescent

INTRODUCTION

Many South African adolescents come from poor socioeconomic environments (Plessis et al. 2007) and are at increased risk of neurodevelopmental delay and lasting neurocognitive dysfunction by way of complex interactions between exogenous and biological factors (Jensen et al. 2017). Exogenous factors include poorer quality of education, lack of social support, greater exposure violence and psychological stressors, whereas biological factors include processes involved in neural growth, energy metabolism, inflammation, and neuroendocrine stress responses (Jensen et al. 2017). However, just how this complex interplay affects neurodevelopment and later functioning remains uncertain.

Epigenetic processes function as an interface between an individual’s environment and molecular biology. Epigenetic regulation is an important aspect of neurodevelopment and cell differentiation, by which biological changes can be elicited by environmental factors, thus making it a potential mechanism for understanding how early life environmental events and realities affect later neurobehavioral and neurophysiological phenotypes (Urdinguio et

al. 2009; Rangasamy et al. 2013; Gapp et al. 2014; Roubroeks et al. 2017). Among known epigenetic processes, DNA methylation (DNAm) plays a particularly critical role in the neurobiology, from the development of the mammalian brain (Jaenisch and Bird 2003) to neurogenesis in adulthood (Simmons et al. 2013; Gapp et al. 2014). There is an ever growing account of the impact of early life events on DNAm; for example, specific DNAm changes have been implicated in the neuropathogenesis of psychiatric illness as a result of prenatal nutrition and exposure to teratogens, prenatal stress, maternal care, early traumatic experiences, and lack of environmental enrichment (Kofink et al. 2013; Turecki and Meaney 2016; Garg et al. 2018)(Gapp et al. 2014; Smigielski et al. 2020).

Based on the established links between early environment and later neurologic and psychiatric outcomes via DNAm, as well as the capacity to now accurately measure DNAm on a genome-wide level, DNAm analysis among phenotypically well-characterized cohorts has potential for deepening our understanding of the neurodevelopmental and cognitive effects of early life adversity and environmental challenges. This has particular relevance among youth in low household income countries such as South Africa who are likely have a significant environmental component in their brain development and later cognitive functioning. Further, the utility of epigenetics extends beyond its explanatory power, as pharmaceutical interventions that could involve manipulation of epigenetic processes such as DNAm may be possible (Xu et al. 2012; Kane and Sinclair 2019).

Several independent groups have demonstrated the potential value one particular type of DNAm biomarker termed *epigenetic clocks* for understanding how environment and disease affect biological aging. For example, applying an early epigenetic clock(Horvath et al. 2016), we and others have shown across numerous data sets that plasma HIV infection accelerates aging in peripheral blood mononuclear cells and brain tissue (Levine et al. 2016; Horvath et al. 2018) and that this accelerated aging is associated with greater likelihood of cognitive dysfunction (Horvath et al. 2018). Our group has also recently demonstrated that age acceleration, as determined via an epigenetic clock, is associated with poorer cognitive functioning in South African adolescents living with HIV (Horvath et al. 2018). However, it remains unknown whether age acceleration is related to alterations in the development of brain structures in otherwise healthy young adolescents. In the current study, we aimed to apply pan tissue epigenetic clocks (Horvath 2013) to a cohort of South African young adolescents to investigate whether accelerated aging is associated with changes in cognitive function, brain macrostructure or white matter integrity. We hypothesised that accelerated aging according to one or more of the epigenetic clocks would be associated with altered neuro-developmental trajectories in adolescents, and that this will be detectable at the macro and microstructure levels of brain anatomy.

METHODS

Participants

A cross-sectional analysis of enrollment data from a neurologic sub study of the Cape Town Adolescent Antiretroviral Cohort (CTAAC), a longitudinal study of adolescents in Cape Town, South Africa was done. The CTAAC study aims to investigate markers of chronic disease processes and progression in five key areas (general adolescent development,

neurocognitive function, pulmonary disease, cardiovascular function, and musculoskeletal disease) in perinatally HIV infected adolescents on ART and healthy adolescents (Hoare et al. 2018). The present study included only the healthy adolescents from this cohort. Routine care providers told all adolescent/caregiver dyads attending one of the 4 recruitment sites, who were in the target age range, about the study. Interested adolescents/caregivers were formally screened, and if eligible and willing to participate, provided with an appointment to attend an enrollment visit 1–2 weeks later at Red Cross War Memorial Children's Hospital. Adolescents were recruited primarily from primary care sector health care service from across Cape Town; inclusion criteria were aged 9–12 years. Exclusion criteria for the present study were: 1) HIV infection 2) an uncontrolled medical condition, such as diabetes mellitus, epilepsy, or tuberculosis (TB) requiring hospital admission; 3) an identified CNS condition, including meningitis (TB or bacterial), cerebrovascular accident, lymphoma, history of head injury with loss of consciousness greater than 5 minutes or any radiological evidence of skull fracture, history of perinatal complications including hypoxic ischemic encephalopathy or neonatal jaundice requiring exchange transfusion, or neurodevelopmental disorder 4) no consent and assent obtainable.

The primary caregiver of each adolescent provided written informed consent prior to participation, and child assent was obtained. The study was approved by the University of Cape Town's Faculty of Health Sciences Human Research Ethics Committee and the University of California Los Angeles Institutional Review Board. Data and samples were obtained from 44 healthy participants between 2013 and 2015. Baseline health and sociodemographic questionnaires were administered to obtain general health information, medical history, and data on ancestry. Pubertal development was measured using the Tanners scale (Micklesfield et al. 2014). Low level systemic inflammation was measured using high sensitivity CRP (hs-CRP) from blood draw.

Stressors and Mental Health Symptoms

Without a formalised stress measure, we combined measures that measure internalised and externalised behaviour and environmental stressors. Caregiver depression was measured using the Center for Epidemiological Studies-Depression (CES-D) (Brenner and Penzenik 2017). Beck Youth Inventories (BYI) (Steer et al. 2016) was used to assess the adolescents' experience of depression, anxiety, anger, disruptive behaviour, and self-concept (Hoare et al. 2019). Child Behaviour Checklist (CBCL) (Louw et al. 2016) was used to assess child behavioural and emotional problems and psychopathology. The life events questionnaire (LEQ) (Roy and Perry 2004) focuses on stressful life events. A stress measure was created by combining CBCL Total Problems, LEQ, Parental depression (CESD) and BYI total score. Higher scores on both the CBCL and the BYI have been associated with stress in children in previous studies (Osika et al. 2007; Kieffer-Kristensen et al. 2011).

Neurocognitive assessment

Each participant was assessed using a battery of standardized neurocognitive tests used in paediatric neuropsychological assessment and research in South Africa (Hoare et al. 2016). Tests were administered in the children's home language. Test instructions were translated and back-translated into isiXhosa, and test administration complied with International Test

Commission guidelines (Muñiz et al. 2013). Where possible neurocognitive measures were adjusted for age by using age-adjusted scaled scores in the scoring of the tests. General intellectual functioning was measured using the Wechsler Abbreviated Scale of Intelligence (WASI: (Axelrod:2002)). The following tests were used to examine cognitive domains: Fingertip Tapping subtest from the NEPSY-II (Brooks et al. 2009). Grooved Pegboard Test (Bryden and Roy 2005). Subtests from the Wechsler Intelligence Scale for Children (WISC-IV; (Wechsler 2003)) measured information processing speed, The Rey Complex Figure Test (RCFT(Watanabe et al. 2005), the Boston Naming Test – Short Form-South Africa (BNT-SF-SA(Roth 2011), category and phonemic fluency, immediate and delayed recall trials of the RCFT and the Hopkins Verbal Learning Test-Revised (HVLT-R: (Benedict et al. 1998), WISC-IV Digit Span backwards (DS backwards) subtest, the Color Trails Test 2 (CTT2) and the NEPSY-II Inhibition subtests.

Cognitive domains

Using data from the test battery, as well as theoretical knowledge about the construct(s) of each test; we created ten separate composite cognitive domains: general intellectual functioning, attention, working memory, visual memory, verbal memory, language, visual spatial ability, motor coordination, processing speed, and executive function. To determine the statistical strength of each cognitive domain, we conducted Cronbach's alpha on combinations of neuropsychological tests to determine which neuropsychological tests had strong inter-relatedness (or internal consistency) within a specific domain. For the Cronbach's alpha, we used the total scaled scores of the tests, and/or subtests, for each of the individual neuropsychological tests. Scaled scores were used because they take into account the child's age and sex. To calculate the individual test scaled scores, the individual test publisher norms were used. Where test publisher norms were not available we converted the test raw score into a z-score. A Cronbach's alpha value of 0.7 was considered an indication of good inter-relatedness between the tests. The Cronbach's alpha were done for domains in which there were more than one neuropsychological test measuring performance within the domain. The domains of language and visual spatial ability, consisted of one test from the battery, and therefore Cronbach's alpha values were not reported for these domains. Tests which did not contribute well to the cognitive domains with regard to the Cronbach's alpha value were excluded from the individual composite cognitive domain scores. Composite cognitive domain scores were calculated by averaging the scores of the all tests that comprised each domain, giving a single score for each domain for individual participants (Phillips et al. 2018). We used the sample's means and standard deviations to convert all scaled and T-scores of the individual neuropsychological tests into z-scores.

Epigenetic Characterization

Blood Collection and Processing—Blood samples were drawn at the enrollment visit. DNA was extracted from blood samples using the QIAsymphony DSP DNA Midi kit and protocol. DNA was quantified using BioDrop (Whitehead Scientific, South Africa) and normalized to a concentration of 5–10ng/ul. All samples were tracked using a Laboratory Information Management System (LIMS; Freezerworks, USA).

DNA Methylation—DNA methylation analysis was performed with the Illumina Infinium Methylation EPIC BeadChip, which measures bisulfite-conversion-based, single-CpG resolution DNAm levels at 866,836 CpG sites in the human genome. The standard protocol of Illumina methylation assays quantifies methylation levels by the β value using the ratio of intensities between methylated (signal A) and un-methylated (signal B) alleles. Specifically, the β value is calculated from the intensity of the methylated (M corresponding to signal A) and un-methylated (U corresponding to signal B) alleles, as the ratio of fluorescent signals β = Max(M,0)/[Max(M,0) + Max(U,0) + 100]. Thus, β values range from 0 (completely un-methylated) to 1 (completely methylated)(Dunning et al. 2008). We used the noob normalization method (Triche et al. 2013), which is implemented in the "minfi" R package (Aryee et al. 2014).

DNA methylation age and the epigenetic clock—Several highly accurate epigenetic biomarkers of chronological age have been proposed (Garagnani et al. 2012; Horvath 2013). These biomarkers use weighted averages of methylation levels at specific CpG sites to produce estimates of age (in units of years), referred to as "DNA methylation age" (DNAm age) or "epigenetic age". Even after adjusting for chronological age, the DNAm age of blood has been found to be associated with the risk for all-cause mortality (Christiansen et al. 2015; Perna et al. 2016), frailty,(Breitling et al. 2016) and cognitive functioning (Chouliaras et al. 2018). We employed two different epigenetic age estimators. First, we used the pan tissue DNAm age estimator(Horvath 2013), which is defined as a prediction method of age based on the DNAm levels of 353 CpGs. Second, we applied the Hannum measure of DNAm age based on 71 CpGs, which was developed using DNA methylation data from blood (Armstrong et al. 2017). After adjusting DNAm age for chronological age, a measure of epigenetic age acceleration is derived. Here we focus on two widely used measures of epigenetic age acceleration denoted by Age acceleration residual *(AAR)* and Extrinsic epigenetic age acceleration *(EEAA),* respectively. By definition, both measures are independent of chronological age (at the time of blood draw). For both measures of age acceleration, positive values indicate that the blood sample is older than expected based on chronological age. AAR is defined as the (raw) residual resulting from regressing the pan tissue DNAm age estimate on chronological age. EEAA can be interpreted as an enhanced version of the Hannum measure of DNAm age estimator because it up-weights the contributions of age-related blood cell counts (Horvath et al. 2016).

The EEAA measure has exhibited the strongest predictive association with all-cause mortality and it revealed the strongest association with cognitive functioning measures in our previous study(Horvath et al. 2018). AAR is less confounded by changes in blood cell composition, applies to all tissue samples, is particularly accurate in adolescents(Horvath 2013; Levine et al. 2016). While AAR is relatively robust with respect to changes in blood cell composition, EEAA capitalizes on age related changes in blood cell types and captures aspects of immunosenescence (Chen et al. 2016).

The epigenetic clock method and software applies to data generated using any Illumina platform (including the EPIC array). Missing CpG probes were automatically imputed by the software. Mathematical details and software tutorials for the epigenetic clock can be

found in the Additional files of (Horvath 2013). An online age calculator can be found at our webpage: http://labs.genetics.ucla.edu/horvath/dnamage/.

Neuroimaging

Image acquisition—Structural and Diffusion weighted imaging was performed at the Cape Universities Brain Imaging Centre on a 3T Siemens Allegra scanner(Hoare et al. 2018). A single-channel transmit-receive head coil was used with the following parameters: TR = 8800ms, TE = 88ms, field-of-view of 220mm, 1.8 × 1.8 × 2.0 mm^3 image resolution, 65 slices, 0% distance factor and 2x GRAPPA acceleration. Images were acquired in an axial orientation with 30 gradient directions at b = 1000mm/s^2, and 3 directions with b = 0mm/s^2. The acquisition was repeated 3 times to allow for redundancy in data. A multi-echo MPRAGE T1-weighted image was acquired with the following parameters: FOV = 256 × 256mm, TR = 2530ms, TE = 1.53/3.21/4.89/6.57ms, TI = 1100ms, flip angle = 7°, 144 slices, in-plane resolution = 1.3 × 1.0mm^2 and slice thickness of 1.0mm.

DTI Preprocessing—Diffusion weighted images were corrected for eddy current distortion within FSL 5.0.1 and imported into MATLAB R2013b for processing. This entailed the affine registration to the average b= 0mm/s^2 image of the first acquisition. For each of the acquisitions, outlier data points were determined by calculating the Z-values at the 25^{th} and 75^{th} percentile of the registered diffusion image. Any data points that were 3 SD from the mean were excluded. The corrected images were exported to FSL 5.0.1 after correction. In FSL 5.0.1 images underwent BET to remove any non-brain tissue and fit a linear tensor model to produce fractional anisotropy (FA) and mean diffusivity (MD) and radial diffusivity (RD) maps.

Fractional anisotropy images were analysed with the TBSS pipeline (Smith et al. 2006). Each participant's FA was registered to a study-specific target. This target was determined by registering each participant to every other participant. The mean square displacement coefficient of each image was calculated and the participant with the lowest mean displacement was chosen as a representative target for the group. After registration to the study-specific target, each image was then up-sampled to MNI space, taking into account the previous transformation parameters. An average FA was created and thinned to produce a mean FA skeleton with a threshold of 0.2. This skeleton is representative of the centres of white matter tracts common to the group. Registration and skeleton projection were also applied to the MD, images as described above.

Freesurfer preprocessing—T1-weighted images were processed with Freesurfer V5.3 on the Lengau cluster at the Centre for High Performance Computing (CHPC), Rosebank, Cape Town, South Africa. The pipeline has been described previously (Fischl et al. 2001). T1-weighted images were normalized, bias-field corrected and skull-stripped. Inner and outer cortical surfaces were modeled as triangular tessellation. Cortical thickness measurements were obtained by calculating the distance (in mm) between pial and grey-white matter surfaces at each vertex location (Fischl and Dale 2000). Cortical surface area was calculated as the average of the grey matter vertices over regions. The vertex data was normalized to the "fsaverage" template included with Freesurfer by utilizing a curvature

matching technique (Fischl et al. 2002). For volumetric data, the brain was segmented into volume-based labels utilizing probabilistic methods (Fischl et al. 2001). After reconstruction, each individual scan was checked for any major errors in segmentation, corrected and rerun if needed.

Statistical analysis

Bivariate Pearson correlation tests were run between the two epigenetic aging measures and 10 cognitive functioning domains, to assess for differences in cognitive performance as epigenetic aging increases. To assess the roles of epigenetic age acceleration on brain structure, we developed backward elimination stepwise multiple regression models in R (version 3.4.3, 2017) covering cortical surface area, cortical thickness, and volume, as well as DTI (FA, MD, RD, and AD) values. Each brain measure was modelled as a dependent variable of a multivariable regression model. The backward feature elimination procedure started out with the full regression model that included all predictors (including chronological age, sex, and epigenetic age acceleration). This was done in order to assess which variables were most associated with brain structural values, leaving only those variables in the model that contributed to the anatomical variance. EEAA and AAR were tested separately to avoid multi-collinearity in the regression models.

In each case, sex, chronological age, and AAR or EEAA were modelled as predictor variables with the value of the regional brain characteristic (i.e. thickness, surface area, volume, FA, or MD) as the dependent (outcome) variable. Each brain region and characteristic led to a separate regression model. Given the stepwise approach (backward feature elimination) taken in the multiple regression analyses, all predictors that had a predictive value of $p<0.15$ were left in the model and thus contribute to the final R^2 value, however, only those that had significant predictive value (nominal $p<0.05$) are in bold typeface in the results tables (Tables 2 and 3). The inclusion of each predictor variable is indicated by its beta value in the relevant column of the results tables. The R^2 values indicate the percentage of the brain characteristic variance explained by each model.

Stepwise general linear models were created to assess effects of pubertal development, hs-CRP, and stress on epigenetic aging measures. Level of pubertal development was also compared between boys and girls.

RESULTS

Demographics

The mean chronological age of the group (n=44) was 10.72 years, with a median age of 10.67 and a DNAm age of 13.83. Ten participants were aged 9, sixteen participants were aged 10, twelve participants were aged 11, six participants were aged 12 years (Table 1A). All of the participants came from low income households. When comparing girls and boys (Table 1B), girls had a higher Tanner score (girls mean=2.04, SD=.81; boys mean=1.17, SD=.38; $p<.001$). Girls and boys chronological ages were not significantly different (girls mean=10.78, SD=1.02; boys mean=10.64, SD=1.00; $p=0.65$). In addition there were no significant differences between girls and boys in DNAm age, AARR, EEAA, hs-CRP and

the combined stress measure. Chronological age was strongly correlated with DNAm Age (r=.52, p<0.001).

Accelerated aging and cognitive performance

Two cognitive domains were negatively associated with higher epigenetic aging in one of the aging measures (EEAA), namely visual memory and visual spatial acuity. AAR was not associated with changes in any of the cognitive domains.

Regression modelling

The results of the regression analyses showed many brain regions had altered structural characteristics associated with epigenetic age.

AAR was associated with decreased cortical thickness in the cingulate, temporal pole, and parahippocampal gyrus. It was also associated with microstructural alterations in RD, MD, and AD values across much white matter, including the internal capsule, fornix, longitudinal and fronto-occipital fasciculi. (Table 2).

EEAA was also associated with many regional structural changes across the brain. Increased EEAA is associated with reduced cortical thickness in the parietal - temporal nexus, as well as medial areas such as the pericalcarine, and fusiform gyri. Surface area across the whole brain was affected negatively by EEAA, while volume in primarily subcortical regions was negatively affected. FA was also negatively affected by EEA, and MD and RD were increased in multiple white matter regions (Table 3).

Sex was positively associated with cortical surface area and FA across a number of brain regions indicating a higher value in females, while MD and RD white matter inflammation markers were lower in females. (see Figure 2) The epigenetic aging markers (AAR and EEAA) contributed more to the brain structural values than biological age, particularly EEAA as a negative contributor of volume, surface area, and cortical thickness, and FA. Overall, EEAA was associated with more alterations in both grey and white matter values than AAR. See Table 2 for full results of AAR and Table 3 for full results of the EEAA models.

Combined Stress score, Tanner score, and hs-CRP were included as predictors in a multiple regression model to predict epigenetic aging, separately for AAR and EEAA. In the model predicting AAR, stress was the only significant predictor variable (F=5.16; p=.029). Pubertal development and hs-CRP were not significant predictors. In the EEAA model, none of the independent variables were significant predictors. T-tests detected no differences between boys and girls in stress (t=−1.56, p=.13), hs-CRP (t=1.29, p=.20), and epigenetic aging (AAR t=−.99, p=.33; EEAA t=−.22, pp=.83).

DISCUSSION

This is the first study to show that epigenetic age acceleration in young adolescents from low income households is associated with alterations in brain morphology and poorer visual memory and visual spatial acuity. Specifically, epigenetic age acceleration (AAR)(Horvath

2013) and extrinsic epigenetic age acceleration (EEAA) were associated with regional decreases in cortical thickness and cortical surface area as well as subcortical grey matter volumes. In addition, white matter microstructural integrity of the internal capsule, superior fronto-occipital and longitudinal fasciculi, and other regions were associated with AAR and EEAA. The epigenetic aging markers (AAR and EEAA) contributed more to the brain structural values than chronological age, particularly EEAA as a negative contributor of volume, surface area, and cortical thickness, and FA. Finally, Stress was a significant predictor of AAR.

Limited research is available on the interaction of epigenetic age and brain macro and microstructure in children or adolescents. Gene expression is regulated through epigenetic mechanisms, for example DNAm, which acts at the interface between environmental stimuli and molecular, cellular and behavioural phenotypes acquired during periods of high developmental plasticity (Fagiolini et al. 2009). Early supportive parenting has a positive effect on the development of a healthy hippocampus, a brain structure important to memory and stress modulation, as previously documented in school children (Luby et al. 2012). Adolescents who grow up in poor socioeconomic conditions could have higher baseline glucocorticoid levels, in addition to adolescents whose caregivers were depressed in the early postnatal period (Lupien et al. 2009). In the current study of young adolescents from low-income households, stress was a significant predictor of AAR. Alterations in grey matter volume and the white matter integrity of the frontal cortex, in addition to reduced volume of the anterior cingulate cortex, has been reported in adolescents exposed to early life adversity (Cohen et al. 2006). The relevance of these findings is underscored by our recent findings adolescents living with HIV, that EEAA remained negatively associated with executive functioning, working memory and processing speed in our cohort, after adjusting for educational level, ethnicity, and household income (Horvath et al. 2018). Thus, accelerated aging and the resulting gradual neurological changes have as their endpoint measurable neurocognitive deficits, which translate into poorer scholastic functioning. One would perhaps not expect DNAm age of blood to be associated with measures of cognitive functioning this early in adolescent neurodevelopment (Horvath et al. 2018). However, the developmental consequences of childhood poverty are well documented (Jensen et al. 2017). A multitude of risk factors are associated with poverty and could have a negative impact on adolescent development. Risks factors that are likely to play a significant role in the adverse developmental effects of poverty include, infectious disease, food insecurity and stressors related to the rearing environment (Jensen et al. 2017). Understanding the contributing factors to cognitive impairment is important, as minor impairments may progress to more significant complications that will influence future functional performance, job opportunities, and community participation of South African youth (Horvath et al. 2018). Importantly, our findings provide further evidence that blood is a potential surrogate for brain tissue when studying neurocognitive impairment (Horvath 2013).

Several limitations of this study should be emphasized. First, the cross-sectional design limits causal inferences and the study number is small. Longitudinal follow-up is underway to better understand the impact of epigenetic age acceleration on brain structure and functioning in later adolescence. Although congenital infections and incidental CNS abnormalities were excluded as far as possible on history, clinical examination and on

clinical review of the MRI scans, it remains a possibility that there may be some overlapping effects of undiagnosed conditions. Future research should focus on delineating specific factors that may account for accelerated aging in adolescence.

Conclusion

This is the first cohort study to examine the relationship between epigenetic age acceleration in blood and various measures of brain structure and cognition in healthy adolescents. Longitudinal follow-up of our cohort will be crucial for determining the ongoing and progressive impact of epigenetic aging. Correlates of epigenetic aging need to be further elucidated, including associations with blood biomarkers, as well as cognition and behaviour in order to understand their impact on the long-term development of neurocognitive disorders.

Acknowledgments

Financial support

This study was funded primarily by R21MH107327-01 (AJL and JH)

Funding for CTAAC provided by R01-HD074051 (HJZ) and SA MRC

HJZ and DJS are supported by the South African Medical Research Council

Funding: This study was funded primarily by R21MH107327-01

Funding for CTAAC provided by R01-HD074051

REFERENCES

Armstrong NJ, Mather KA, Thalamuthu A, et al. (2017) Aging, exceptional longevity and comparisons of the Hannum and Horvath epigenetic clocks. Epigenomics 9:689–700. doi: 10.2217/epi-2016-0179 [PubMed: 28470125]

Aryee MJ, Jaffe AE, Corrada-Bravo H, et al. (2014) Minfi: a flexible and comprehensive Bioconductor package for the analysis of Infinium DNA methylation microarrays. Bioinformatics 30:1363–1369. doi: 10.1093/bioinformatics/btu049 [PubMed: 24478339]

Benedict RHB, Schretlen D, Groninger L, Brandt J (1998) Hopkins Verbal Learning Test? Revised: Normative Data and Analysis of Inter-Form and Test-Retest Reliability. The Clinical Neuropsychologist (Neuropsychology, Development and Cognition: Section D) 12:43–55. doi: 10.1076/clin.12.1.43.1726

Breitling LP, Saum K-U, Perna L, et al. (2016) Frailty is associated with the epigenetic clock but not with telomere length in a German cohort. Clinical Epigenetics 8:1186. doi: 10.1186/s13148-016-0186-5

Brenner LA, Penzenik M (2017) Center for Epidemiological Studies-Depression. In: Encyclopedia of Clinical Neuropsychology Springer International Publishing, Cham, pp 1–3

Brooks BL, Sherman EMS, Strauss E (2009) NEPSY-II: A Developmental Neuropsychological Assessment, Second Edition. Child Neuropsychology 16:80–101. doi: 10.1080/09297040903146966

Bryden PJ, Roy EA (2005) Unimanual performance across the age span. Brain Cogn 57:26–29. doi: 10.1016/j.bandc.2004.08.016 [PubMed: 15629210]

Chen BH, Marioni RE, Colicino E, et al. (2016) DNA methylation-based measures of biological age: meta-analysis predicting time to death. Aging (Albany NY) 8:1844–1865. doi: 10.18632/aging.101020 [PubMed: 27690265]

Chouliaras L, Pishva E, Haapakoski R, et al. (2018) Peripheral DNA methylation, cognitive decline and brain aging: pilot findings from the Whitehall II imaging study. Epigenomics 10:585–595. doi: 10.2217/epi-2017-0132 [PubMed: 29692214]

Christiansen L, Lenart A, Tan Q, et al. (2015) DNA methylation age is associated with mortality in a longitudinal Danish twin study. Aging Cell 15:149–154. doi: 10.1111/acel.12421 [PubMed: 26594032]

Cohen RA, Grieve S, Hoth KF, et al. (2006) Early life stress and morphometry of the adult anterior cingulate cortex and caudate nuclei. Biol Psychiatry 59:975–982. doi: 10.1016/j.biopsych.2005.12.016 [PubMed: 16616722]

Dunning MJ, Barbosa-Morais NL, Lynch AG, et al. (2008) Statistical issues in the analysis of Illumina data. BMC Bioinformatics 9:85. doi: 10.1186/1471-2105-9-85 [PubMed: 18254947]

Fagiolini M, Jensen CL, Champagne FA (2009) Epigenetic influences on brain development and plasticity. Curr Opin Neurobiol 19:207–212. doi: 10.1016/j.conb.2009.05.009 [PubMed: 19545993]

Fischl B, Dale AM (2000) Measuring the thickness of the human cerebral cortex from magnetic resonance images. Proceedings of the National Academy of Sciences 97:11050–11055. doi: 10.1073/pnas.200033797

Fischl B, Salat D, Kennedy D, et al. (2001) Automatic segmentation of the structures in the human brain. Neuroimage 13:118. doi: 10.1016/S1053-8119(01)91461-2

Fischl B, Salat DH, Busa E, et al. (2002) Whole brain segmentation: automated labeling of neuroanatomical structures in the human brain. Neuron 33:341–355. [PubMed: 11832223]

Gapp K, Woldemichael BT, Bohacek J, Mansuy IM (2014) Epigenetic regulation in neurodevelopment and neurodegenerative diseases. Neuroscience 264:99–111. doi: 10.1016/j.neuroscience.2012.11.040 [PubMed: 23256926]

Garagnani P, Bacalini MG, Pirazzini C, et al. (2012) Methylation of ELOVL2gene as a new epigenetic marker of age. Aging Cell 11:1132–1134. doi: 10.1111/acel.12005 [PubMed: 23061750]

Garg E, Chen L, Nguyen TTT, et al. (2018) The early care environment and DNA methylome variation in childhood. Development and Psychopathology 30:891–903. doi: 10.1017/S0954579418000627 [PubMed: 30068421]

Hoare J, Fouche J-P, Phillips N, et al. (2018) Structural brain changes in perinatally HIV infected young adolescents in South Africa. AIDS 1. doi: 10.1097/QAD.0000000000002024

Hoare J, Phillips N, Brittain K, et al. (2019) Mental Health and Functional Competence in the Cape Town Adolescent Antiretroviral Cohort. J Acquir Immune Defic Syndr 81:e109–e116. doi: 10.1097/QAI.0000000000002068 [PubMed: 31241543]

Hoare J, Phillips N, Joska JA, et al. (2016) Applying the HIV-associated neurocognitive disorder diagnostic criteria to HIV-infected youth. Neurology 87:86–93. doi: 10.1212/WNL.0000000000002669 [PubMed: 27206720]

Horvath S (2013) DNA methylation age of human tissues and cell types. Genome Biol 14:R115. doi: 10.1186/gb-2013-14-10-r115 [PubMed: 24138928]

Horvath S, Gurven M, Levine ME, et al. (2016) An epigenetic clock analysis of race/ethnicity, sex, and coronary heart disease. Genome Biol 17:171. doi: 10.1186/s13059-016-1030-0 [PubMed: 27511193]

Horvath S, Phillips N, Heany SJ, et al. (2018) Perinatally acquired HIV infection accelerates epigenetic aging in South African adolescents. AIDS 1. doi: 10.1097/QAD.0000000000001854

Jaenisch R, Bird A (2003) Epigenetic regulation of gene expression: how the genome integrates intrinsic and environmental signals. Nat Genet 33 Suppl:245–254. doi: 10.1038/ng1089 [PubMed: 12610534]

Jensen SKG, Berens AE, Nelson CA 3rd (2017) Effects of poverty on interacting biological systems underlying child development. The Lancet Child & Adolescent Health 1:225–239. doi: 10.1016/S2352-4642(17)30024-X

Kieffer-Kristensen R, Teasdale TW, Bilenberg N (2011) Post-traumatic stress symptoms and psychological functioning in children of parents with acquired brain injury. Brain Injury 25:752–760. doi: 10.3109/02699052.2011.579933 [PubMed: 21604930]

Kofink D, Boks MPM, Timmers HTM, Kas MJ (2013) Epigenetic dynamics in psychiatric disorders: Environmental programming of neurodevelopmental processes. Neuroscience & Biobehavioral Reviews 37:831–845. doi: 10.1016/j.neubiorev.2013.03.020 [PubMed: 23567520]

Levine AJ, Quach A, Moore DJ, et al. (2016) Accelerated epigenetic aging in brain is associated with pre-mortem HIV-associated neurocognitive disorders. J Neurovirol 22:366–375. doi: 10.1007/s13365-015-0406-3 [PubMed: 26689571]

Louw K-A, Ipser J, Phillips N, Hoare J (2016) Correlates of emotional and behavioural problems in children with perinatally acquired HIV in Cape Town, South Africa. AIDS Care 1–9. doi: 10.1080/09540121.2016.1140892

Luby JL, Barch DM, Belden A, et al. (2012) Maternal support in early childhood predicts larger hippocampal volumes at school age. Proc Natl Acad Sci USA 109:2854–2859. doi: 10.1073/pnas.1118003109 [PubMed: 22308421]

Lupien SJ, McEwen BS, Gunnar MR, Heim C (2009) Effects of stress throughout the lifespan on the brain, behaviour and cognition. Nat Rev Neurosci 10:434–445. doi: 10.1038/nrn2639 [PubMed: 19401723]

Micklesfield LK, Pedro TM, Kahn K, et al. (2014) Physical activity and sedentary behavior among adolescents in rural South Africa: levels, patterns and correlates. BMC Public Health 14:1–10. doi: 10.1186/1471-2458-14-40 [PubMed: 24383435]

Muñiz J, Elosua P, Hambleton RK, International Test Commission (2013) [International Test Commission Guidelines for test translation and adaptation: second edition]. Psicothema 25:151–157. [PubMed: 23628527]

Osika W, Friberg P, Wahrborg P (2007) A new short self-rating questionnaire to assess stress in children. Int J Behav Med 14:108–117. doi: 10.1007/BF03004176 [PubMed: 17926439]

Perna L, Zhang Y, Mons U, et al. (2016) Epigenetic age acceleration predicts cancer, cardiovascular, and all-cause mortality in a German case cohort. Clinical Epigenetics 8:6. doi: 10.1186/s13148-016-0228-z [PubMed: 26798409]

Phillips NJ, Hoare J, Stein DJ, et al. (2018) HIV-associated cognitive disorders in perinatally infected children and adolescents: a novel composite cognitive domains score. AIDS Care 30:1–9. doi: 10.1080/09540121.2018.1466982

Plessis Du P, Reviews LCERA, 2007 Children and poverty in South Africa: The right to social security.

Roth C (2011) Boston Naming Test. In: Encyclopedia of Clinical Neuropsychology Springer New York, New York, NY, pp 430–433

Roy CA, Perry JC (2004) Instruments for the Assessment of Childhood Trauma in Adults. J Nerv Ment Dis 192:343–351. doi: 10.1097/01.nmd.0000126701.23121.fa [PubMed: 15126888]

Simmons RK, Stringfellow SA, Glover ME, et al. (2013) DNA methylation markers in the postnatal developing rat brain. Brain Res 1533:26–36. doi: 10.1016/j.brainres.2013.08.005 [PubMed: 23954679]

Smith SM, Jenkinson M, Johansen-Berg H, et al. (2006) Tract-based spatial statistics: voxelwise analysis of multi-subject diffusion data. Neuroimage 31:1487–1505. doi: 10.1016/j.neuroimage.2006.02.024 [PubMed: 16624579]

Steer RA, Kumar G, Beck JS, Beck AT (2016) Evidence for the Construct Validities of the Beck Youth Inventories with Child Psychiatric Outpatients. Psychological Reports 89:559–565. doi: 10.2466/pr0.2001.89.3.559

Triche TJ Jr, Weisenberger DJ, Van Den Berg D, et al. (2013) Low-level processing of Illumina Infinium DNA Methylation BeadArrays. Nucleic Acids Research 41:e90–e90. doi: 10.1093/nar/gkt090 [PubMed: 23476028]

Turecki G, Meaney MJ (2016) Effects of the Social Environment and Stress on Glucocorticoid Receptor Gene Methylation: A Systematic Review. Biol Psychiatry 79:87–96. doi: 10.1016/j.biopsych.2014.11.022 [PubMed: 25687413]

Watanabe K, Ogino T, Nakano K, et al. (2005) The Rey-Osterrieth Complex Figure as a measure of executive function in childhood. Brain Dev 27:564–569. doi: 10.1016/j.braindev.2005.02.007 [PubMed: 16310591]

Wechsler D (2003) Wechsler Intelligence Scale for Children, Fourth Edition.

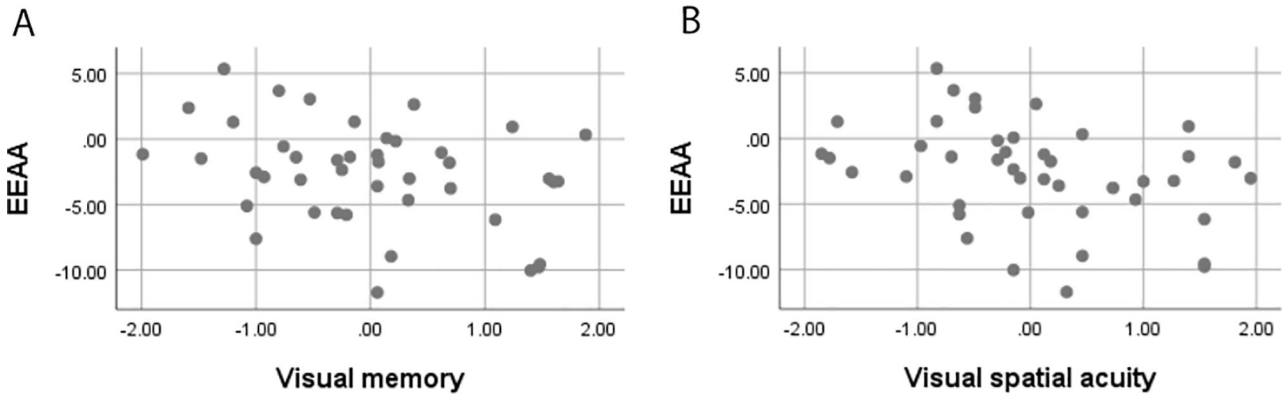

Figure 1.

A. Pearson correlation = −.34, p = .026

B. Pearson correlation = −.36, p = .020

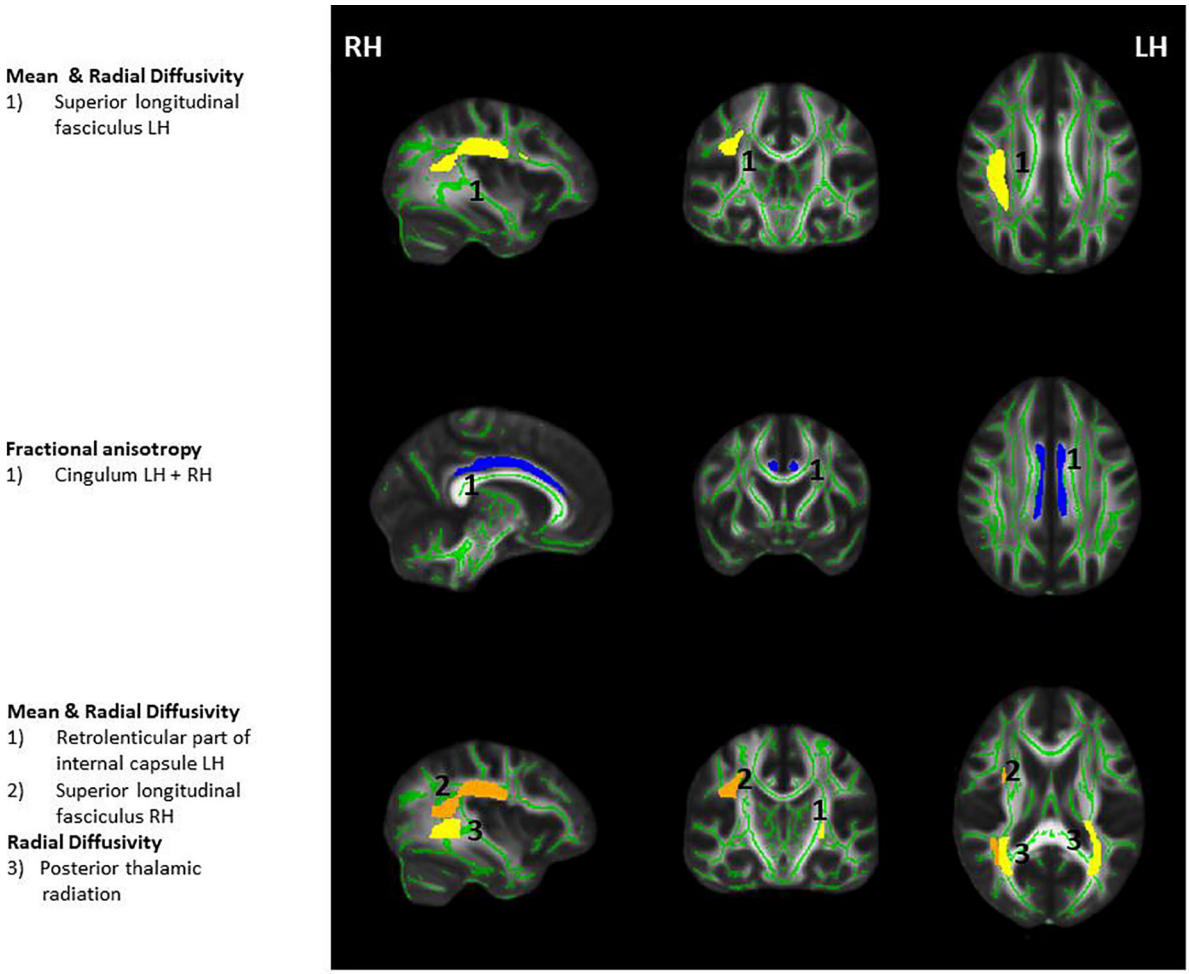

Figure 2:

Significant sex associations with white matter microstructure are shown here ($p < 0.05$). Other predictors in the models included age, EEAA and AAR. For details refer to Table 2 and 3.

Table 1:

Demographic and clinical characteristics. N=44

A			
Age in years: Mean (SD)	10.72(1.00)		
DNAm age	13.83(2.9)		
Gender: Male/Female	19/24		
Ethnicity: Black African/Other	44/0		
Home Language: isiXhosa/Other	42/2		
Low household income: (%)[a]	100%		
B	Boys (n=20)	Girls (n=24)	P value
	Mean(SD)	Mean(SD)	
Age in years	10.64(1.0)	10.78(1.0)	T=−0.4 p=.65
DNAm age	13.31(2.7)	14.25(3.0)	T=−1.1 p=.29
AAR	−2.16(2.3)	−1.41(2.6)	T=−0.9 p=.33
EEAA	−2.79(4.7)	−2.54(3.1)	T=−0.2 p=.83
Tanner score	1.17(.38)	2.04(.81)	T=−4.2 p<0.001
Stress	112.87(19.5)	123.56(24.0)	T=−1.6 p=.13
hs-CRP	3.94(11.3)	0.96(1.0)	T=1.3 p=.20

NOTES:

a: annual household income brackets in ZAR: R0 -R25000 p.a.

Table 2:

Results of AAR and additional predictors on regional brain characteristics

Structural measure	Brain region	Hem.	Sex β(p)	Age β(p)	Age acceleration β(p)	R^2	P
Thickness	Caudal anterior cingulate	L	**.30(.038)**	**.29(.040)**	**−.31(.033)**	.250	.009
	Temporal pole	L			**−.32(.039)**	.100	.039
	Parahippocampal gyrus	R	.25(.069)	**.31(.025)**	**−.41(.004)**	.300	.003
	Rostral middle frontal gyrus	R	−.27(.065)	**−.31(.028)**		.181	.018
FA	Cingulum	R	.40(.064)			.161	.021
MD	Post limb of internal capsule	R			**−.44(.043)**	.189	.043
	Post limb of internal capsule	L			**−.43(.047)**	.182	.048
	Sup longitudinal fasciculus	R	**−.44(.042)**			.191	.042
	Sup fronto occipital fasciculus	R			**.53(.012)**	.278	.018
RD	Post limb of internal capsule	R			**−.45(.034)**	.206	.034
	Fornix stria terminalis	R			−.40(.067)	.158	.067
	Sup longitudinal fasciculus	R	**−.43(.044)**			.188	.044
	Sup fronto occipital fasciculus	R			**.43(.044)**	.188	.044
AD	Cerebral peduncle	R			.14(.055)	.171	.055
	Genu of corpus callosum	n/a		**−.46(.030)**		.214	.030
	Sup fronto occipital fasciculus	R			**.47(.026)**	.223	.026

Standardized beta scores (β) for each predictor variable in each model are shown in the relevant named columns, with p values in parentheses. R^2 values and p values in the final column are for each full model. Each row is one full model. Included covariates that are significant predictors ($p<0.05$) in each model are highlighted in bold.

Table 3:

Results of EEAA and additional predictors on regional brain characteristics

Structural measure	Brain region	Hem.	Sex β(p)	Age β(p)	EEAA β(p)	R^2	P
Thickness	Entorhinal gyrus	L			**−.41(.006)**	.17	.007
	Fusiform gyrus	L			**−.38(.012)**	.15	.012
	Inf parietal gyrus	L			**−.39(.010)**	.15	.009
	Inf temporal gyrus	L			**−.40(.008)**	.16	.009
	Mid temporal gyrus	L			**−.50(.001)**	.25	.001
	Precentral gyrus	L			**−.32(.038)**	.10	.038
	Supramarginal gyrus	L			**−.41(.007)**	.17	.007
	Temporal pole	L			**−.40(.008)**	.16	.008
	Fusiform gyrus	R			**−.31(.047)**	.09	.047
	Mid temporal gyrus	R			**−.31(.045)**	.10	.045
	Pars opercularis	R			**−.31(.045)**	.10	.045
	Pericalcarine	R	**−.34(.014)**		**.43(.002)**	.29	.001
Area	Caudal mid frontal gyrus	L			**−.31(.046)**	.09	.046
	Cuneus	L			**−.40(.007)**	.16	.008
	Fusiform gyrus	L			**−.57(<.001)**	.32	<.001
	Inf temporal gyrus	L			**−.46(.002)**	.21	.002
	Isthmus cingulate	L			**−.402(.010)**	.19	.016
	Lateral occipital	L			**−.65(<.001)**	.43	<.001
	Lat orbitofrontal	L			**−.43(.004)**	.19	.004
	Lingual gyrus	L			**−.50(.001)**	.25	<.001
	Mid temporal gyrus	L			**−.46(.002)**	.21	.002
	Parahippocampal	L			**−.54(<.001)**	.30	<.001
	Pars orbitalis	L			**−.37(.015)**	.14	.016
	Pars triangularis	L			**−.45(.002)**	.21	.002
	Postcentral gyrus	L			**−.48(.001)**	.23	.001
	Precuneus	L			**−.38(.012)**	.14	.012
	White matter surface area	L			**−.53(<.001)**	.28	<.001
	Caudal mid frontal gyrus	R			**−.39(.009)**	.16	.009

Metab Brain Dis. Author manuscript; available in PMC 2021 December 01.

Structural measure	Brain region	Hem.	Sex β(p)	Age β(p)	EEAA β(p)	R^2	P
	Cuneus	R	**.27(.048)**		**−.48(.001)**	.29	.001
	Fusiform gyrus	R			**−.54(<.001)**	.29	<.001
	Inf parietal gyrus	R			**−.34(.027)**	.11	.027
	Inf temporal gyrus	R			**−.42(.005)**	.17	.005
	Isthmus cingulate	R			**−.31(.042)**	.10	.042
	Lat occipital	R			**−.54(<.001)**	.29	<.001
	Lat orbitofrontal	R			**−.48(.001)**	.23	.001
	Lingual	R			**−.58(<.001)**	.34	<.001
	Med orbitofrontal	R			**−.55(<.001)**	.30	<.001
	Parahippocampal	R			**−.44(.003)**	.19	.003
	Pars orbitalis	R			**−.44(.004)**	.19	.004
	Pars triangularis	R			**−.50(.001)**	.25	<.001
	Postcentral	R			**−.49(.001)**	.24	<.001
	Precuneus	R			**−.48(.001)**	.23	.001
	Rostral anterior cingulate	R	**.31(.041)**		−.28(.062)	.16	.028
	Rostral mid frontal	R			**−.50(.001)**	.25	<.001
	Sup frontal	R			**−.44(.004)**	.19	.004
	Sup parietal	R	**.34(.015)**		**−.43(.003)**	.29	.001
	Sup temporal	R			**−.35(.022)**	.12	.022
	Insula	R			**−.33(.031)**	.11	.031
	White matter surface area	R			**−.53(<.001)**	.28	<.001
Volume	Thalamus	L	**−.30(.030)**		**−.44(.002)**	.29	.001
	Caudate	L			**−.32(.037)**	.10	.037
	Pallidum	L			**−.38(.011)**	.15	.011
	Amygdala	L			**−.34(.026)**	.11	.027
	Brain stem	n/a			**−.43(.003)**	.27	.002
	Thalamus	R	−.28(.056)		**−.36(.013)**	.22	.008
	Pallidum	R			**−.37(.016)**	.13	.016
	Hippocampus	R			**−.31(.043)**	.10	.044
	Cortex volume	n/a			**−.46(.002)**	.21	.002
FA	Cerebral peduncle	L		**−.39(.024)**	**−.70(<.001)**	.54	<.001

Structural measure	Brain region	Hem.	Sex β(p)	Age β(p)	EEAA β(p)	R^2	P
	Retrolenticular internal capsule	R			**−.43(.048)**	.18	.048
	Retrolenticular internal capsule	L			**−.54(.010)**	.29	.010
	Ant corona radiata	L			**−.52(.012)**	.28	.012
	Post corona radiata	L			**−.50(.018**	.25	.018
	Genu of corpus callosum	n/z		**−.46(.011)**	**−.64(.001)**	.51	.001
	Sagittal striatum	L			**−.47(.028)**	.22	.028
	External capsule	R			**−.60(.003)**	.36	.003
	External capsule	L			**−.62(.002)**	.38	.002
	Cingulum	R	**.41(.035)**		**−.46(.019)**	.38	.011
	Cingulum	L	**.42(.032)**		**−.44(.025)**	.37	.013
	Fornix stria terminalis	R		**−.48(.006)**	**−.67(<.001)**	.56	<.001
	Fornix stria terminalis	L		**−.40(.040)**	**−.59(.004)**	.41	.006
	Sup longitudinal fasciculus	R		**−.41(.013)**	**−.74(<.001)**	.60	<.001
	Fornix	n/a			**−.57(.005)**	.33	.005
MD	Post limb internal capsule	L			**.60(.003)**	.36	.003
	Retrolenticular internal capsule	R			**.49(.021)**	.34	.021
	Retrolenticular internal capsule	L	**−.40(.036)**		**.50(.011)**	.40	.008
	Sup longitudinal fasciculus	R	**−.45(.015)**		**.52(.006)**	.46	.003
	Sup longitudinal fasciculus	L			**.48(.025)**	.23	.025
	Splenium of corpus callosum	n/a			**.45(.037)**	.20	.037
RD	Post internal capsule	L			**.54(.009)**	.30	.009
	Retrolenticular internal capsule	R			**.48(.024)**	.23	.024
	Retrolenticular internal capsule	L	**−.44(.020)**		**.51(.008)**	.44	.004
	Post thalamic radiation	n/a	**−.42(.038)**		.39(.052)	.32	.025
	Sup longitudinal fasciculus	R	**−.45(.008)**		**.62(.001)**	.57	<.001
	Sup longitudinal fasciculus	L			**.50(.019)**	.25	.019
	Splenium of corpus callosum	n/a			**.46(.033)**	.21	.033
AD	Post limb of internal capsule	L			**.57(.005)**	.33	.005
	Genu of corpus callosum	n/a		**−.46(.030)**		.21	.030

Standardized beta scores (β) for each predictor variable in each model are shown in the relevant named columns, with p values in parentheses. R^2 values and p values in the final column are for each full model. Each row is one full model. Included covariates that are significant predictors (p<0.05) in each model are highlighted in bold.